Biosensors and Bioelectronics 25 (2009) 920–926

Contents lists available at ScienceDirect

Biosensors and Bioelectronics

journal homepage: www.elsevier.com/locate/bios

Biosensing at disk microelectrode arrays. Inter-electrode functionalisation allows formatting into miniaturised sensing platforms of enhanced sensitivity

Eva Baldrich*, Fco. Javier del Campo, Francesc Xavier Muñoz

Instituto de Microelectrónica de Barcelona (IMB-CNM), CSIC, Campus Universidad Autónoma de Barcelona, Barcelona 08193, Spain

ARTICLE INFO

Article history:
Received 10 August 2009
Received in revised form 1 September 2009
Accepted 2 September 2009
Available online 9 September 2009

Keywords:
Disk microelectrode array
Sensing platform
Biosensor
HRP detection
H_2O_2 detection
Tetramethylbenzidine (TMB)

ABSTRACT

Biosensor performance depends on the effective functionalisation of a transducer with suitable biorecognition elements. During functionalisation, surface blocking steps are normally carried out to avoid later binding of undesirable molecules and thus guarantee biosensor specificity. However, these blocking steps may be deleterious in electrochemical systems where transduction ultimately relies on electron transfer between the electrode and a redox species in solution. This work presents a novel approach to develop improved amperometric biosensing platforms using microfabricated disk microelectrode arrays, based on the functionalisation of the inert surface surrounding the active microdisks. These devices more than doubled assay sensitivity compared to conventional biosensors produced using the same arrays. This approach benefits from three advantages: the functionalisation of a broader surface, the possibility to activate the microelectrodes immediately before detection, and access to enhanced rates of mass transport to microelectrodes that improve device sensitivity. To demonstrate this, we first studied the electrochemical behaviour of tetramethylbenzidine (TMB) at gold disk microelectrode arrays, and then used TMB as the redox mediator for the amperometric biosensing of HRP/H_2O_2. Down to 0.54 pM H_2O_2 or as little as 25 pM HRP were detected within 5 s of enzyme activity in just 10 μl of enzyme substrate solution. We postulate that microelectrode arrays may be used to develop novel electrochemical biosensing platforms that are faster and more sensitive than conventional biosensors.

1. Introduction

Affinity-based biosensors often need blocking of the transducer surface with inert materials to minimise non-specific signals, because biosensor specificity is only guaranteed in the absence of non-specific adsorption of unwanted components. Bovine serum albumin, BSA, is the protein most widely used for this purpose, and it works by adsorbing on the gaps left among the biorecognition elements used to functionalise the transducer. However, blocking agents may also exert adverse effects in electrochemical systems where signal transduction ultimately relies on electron transfer steps.

Microelectrode arrays are powerful tools in electroanalysis as they allow access to mass transport rates comparable to microelectrodes and current levels similar to macroelectrodes (Ordeig et al., 2006, 2007). The microelectrode arrays used in this work consist of a large number of individual microdisks that are wired in parallel, patterned in a regular lattice over an inert surface and separated from their closest neighbours by a distance several times their diameter. This means that only a small fraction of the whole transducer surface area is at work. In this work we also exploit the electrochemically inert surface of microelectrode arrays to develop immunosensors that are more sensitive than previously reported electrochemical systems. We functionalised the inert part of the arrays and kept the microelectrodes electrochemically active. Electrode passivation could be avoided by electrochemical activation after the various steps in a typical immunoassay. Since the activation only affects the microelectrodes, biomolecules such as enzymes, antibodies or DNA probes could be safely attached to the surface among them.

Here we prove this concept using a well-known electrochemical system based on the enzyme horseradish peroxidase, HRP, and 3,3′,5,5′-tetramethylbenzidine, TMB^0, as the redox mediator. HRP catalyses the oxidation of numerous reducing substrates by hydrogen peroxide (H_2O_2) following the general reaction summarized in Fig. 1a. A variety of HRP substrates have been described, including aromatic phenols, phenolic acids, indoles, amines and sulfonates, which regenerate the enzyme active centre, oxidised as a result of the reaction with H_2O_2 (Regalado et al., 2004; Veitch, 2004). Using reversible redox substrates allows for enhanced electrochemical detection, as the mediator shuttles electrons between the enzyme active site and the electrode. The rate of mediator reduction can then serve to estimate HRP and/or H_2O_2 concentration. Compared with other widely used enzymes like alkaline phosphatase, HRP is

* Corresponding author. Tel.: +34 93 5947700x1306; fax: +34 93 58014 96.
E-mail address: eva.baldrich@imb-cnm.csic.es (E. Baldrich).

0956-5663/$ – see front matter © 2009 Elsevier B.V. All rights reserved.
doi:10.1016/j.bios.2009.09.009

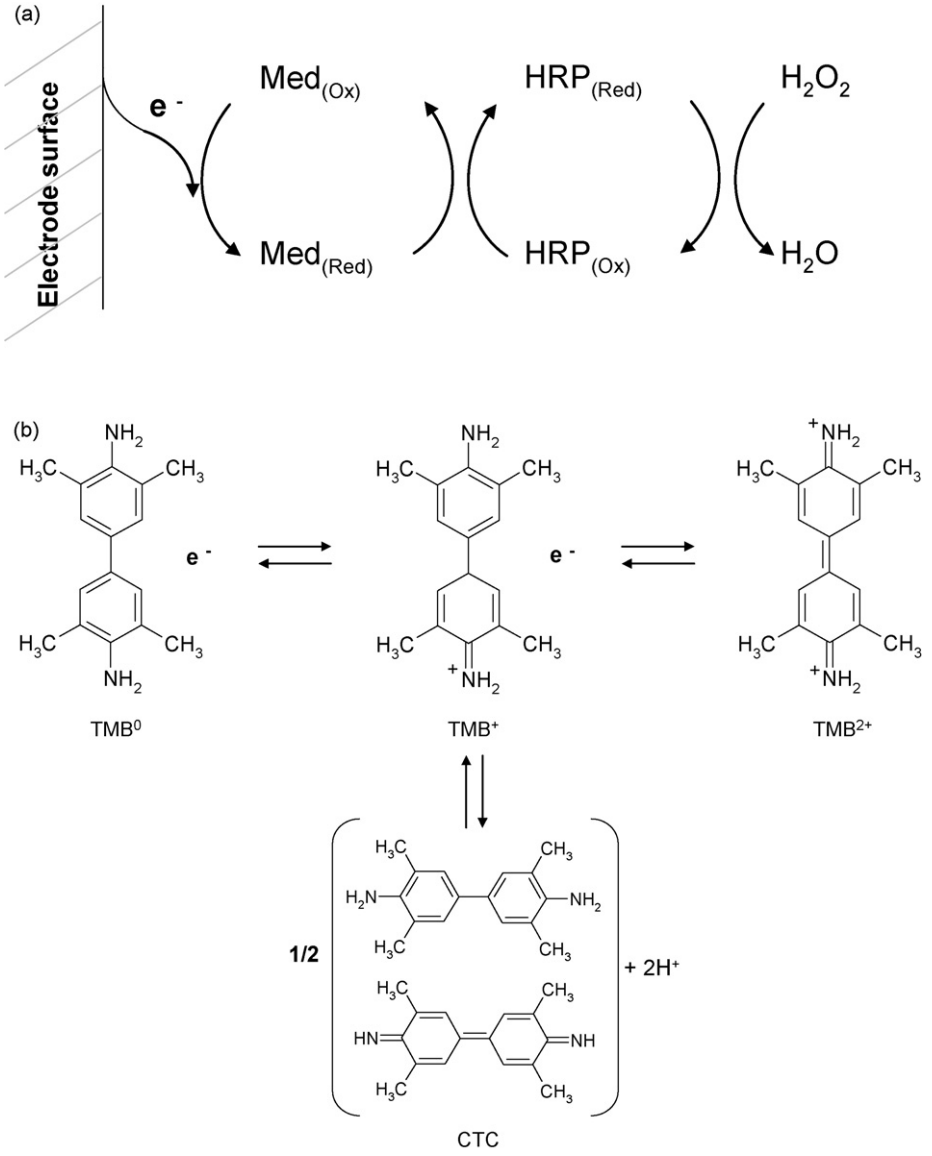

Fig. 1. (a) Reduction of H_2O_2 by a redox mediator catalysed by HRP. (b) TMB^0 electro-oxidation in aqueous solution at neutral pH involves two consecutive one-electron steps. The radical intermediate, TMB^+, coexist in solution with a blue charge-transfer complex, CTC, attributed to the reversible complexation of TMB^0 and TMB^{2+}.

less costly, smaller, more stable and has a high turnover rate that allows the generation of strong signals in a relatively short time. The availability of a variety of substrates has encouraged the use of HRP in the preparation of enzyme-labelled biocomponents, especially in immunohistochemistry and immunoassays (Kricka, 1994; Regalado et al., 2004).

TMB^0 is one of the most widely used chromogenic substrates for HRP-based detection systems and commercial ELISA test kits because it is less toxic and provides higher assay sensitivity and faster reactions than other HRP substrates such as *O*-phenylenediamine (OPD) and 2,2′-azino-bis-(3-ethylbenzthiazoline-6-sulfonic acid) (ABTS). TMB^0 shows in aqueous solution at pH 4.0–7.0 near fully reversible electro-oxidation that involves two consecutive one-electron steps. These are attributed to the formation of a radical intermediate, TMB^+, and a yellow two-electron oxidised product, TMB^{2+}. As shown in Fig. 1b, TMB^+ is present in solution in equilibrium with a charge-transfer complex, CTC (Volpe et al., 1998; Liu et al., 2008). This CTC has been attributed to the reversible complexation of the reduced TMB^0 (a neutral diamine that behaves as the electron donor) and TMB^{2+} (a diimine that behaves as the CTC electron acceptor) (Awano et al., 1990; Misono et al., 1997; Liu et al., 2008). The CTC, which is blue, is also electroactive and presents a single reversible voltammetric peak (Josephy et al., 1982; Liu et al., 2008). Under strong acidic conditions, however, the voltammetry of TMB^0 shows a single two-electron oxidation/reduction wave, because low pHs favour the formation of TMB^{2+} (Misono et al., 1997; Crew et al., 2007; Liu et al., 2008).

The electrochemical monitoring of HRP activity using H_2O_2 and TMB has been successfully applied to ELISA and Enzyme-linked Aptamer Assay (ELAA) detection. Reports exist for chronoamperometry, cyclic voltammetry, differential pulse voltammetry, and square wave voltammetry, often coupled to flow injection analysis (FIA) and nearly always based on macroelectrodes. In these examples, the electrochemical assay format usually shows wider assay dynamic ranges, lower detection limits, and shorter incubation times than the colorimetric counterparts (He et al., 1997, 2003; Draisci et al., 2001; Pyun et al., 2001; Valentini et al., 2003; Baldrich et al., 2005; Fanjul-Bolado et al., 2005; Liu et al., 2005, 2006; Crew et al., 2007). While HRP is one of the most widely used enzymes in biosensing, the use of TMB as the substrate is restricted to a few reports relying on amperometric detection using

functionalised screen-printed and carbon macroelectrodes (Zhou et al., 2003; Butler et al., 2006; Conneely et al., 2007; Lu et al., 2007; Kurtinaitiene et al., 2008; Parker and Tothill, 2009; Salam and Tothill, 2009).

Here we show that microelectrode arrays provide new opportunities in the field of biosensors. To demonstrate this, we first investigate the electrochemical behaviour of TMB as the redox mediator at microdisk electrode arrays. Next, we explore different strategies for HRP/H_2O_2 electrochemical biosensing using these devices. Finally, we show that microelectrode arrays can be functionalised and operated in minute solution volumes, and that their utilization as sensing platforms provides enhanced detectability compared with classical sensing.

2. Material and methods

2.1. Reagents and instrumentation

Bovine serum albumin (BSA), potassium chloride (KCl), potassium ferricyanide ($K_3[Fe(CN)_6]$), hydrogen peroxide (H_2O_2, 30%), 3,3′,5,5′-tetramethylbenzidine dihydrochloride hydrate (TMB, ≥98.0%), and ready-to-use 3,3′,5,5′-tetramethylbenzidine liquid substrate system for ELISA (TMB/H_2O_2 substrate solution) were obtained from Sigma–Aldrich. TMB was dissolved to 20 mM in water, followed by 1:100 dilution in phosphate-citrate buffer, pH 5. Neutravidin, biotinylated HRP and phosphate-buffered saline tablets (PBS, 10 mM PBS, NaCl 13.8 mM; KCl 2.7 mM, pH 7.4) were provided by Invitrogen (Barcelona, Spain). The PBST washing solution was PBS with 0.05% Tween 20 (Sigma). All solutions were prepared using high purity water of conductivity not less than 18 MΩ cm.

Electrochemical measurements were carried out in a Faraday's cage with a μ-Autolab III potentiostat (Eco-Chemie, The Netherlands).

2.2. Electrode fabrication and characterisation

Gold microelectrode arrays were produced using standard photolithographic techniques (Davies et al., 2005). Briefly, a 1 mm thick thermal oxide layer was grown over silicon or pyrex wafers. Wafers were metallised using a triple layer of titanium, nickel and gold, 20, 20 and 150 nm thick respectively, patterned photolithographically in a wet etching step, followed by silicon oxide and silicon nitride deposition to provide electrical insulation of the devices. The final geometry of the arrays, including connection pads, was defined by photolithography in a dry step using reactive ion etching. Finally, the wafers were diced into individual chips which were subsequently mounted, wire bonded and encapsulated onto printed circuit boards. Each device consisted of 182 gold microdisks of 10 μm radius each, separated 100 microns from their nearest neighbours, and arranged in a square lattice over a 1.5 mm × 1.5 mm surface.

Before activation, the chips were washed serially in ethanol, isopropanol and water, and dried under a nitrogen flow. The electrochemical activation consisted in a series of potential pulses (10 s each) from 0 to −2 V *vs* an external Ag/AgCl (3 M KCl) in 0.1 mM KCl. Then the number of active microdisks in each array was determined by cyclic voltammetry in ferricyanide (Ordeig et al., 2006).

2.3. Electrode functionalisation with HRP

Unless otherwise stated, incubations were carried out inside a humid chamber, consisting in a closed container enclosing a damp paper towel, to prevent evaporation and preserve biocomponent's integrity. HRP was immobilised separately by direct physisorption and by affinity capture on active electrodes as follows: HRP was directly physisorbed from a 6 μl drop of biotinylated HRP (0–10 pM in PBS) that was incubated for 15 min at room temperature on the surface of the microelectrode arrays. For HRP immobilisation by affinity capture, a 6 μl drop of neutravidin 20 μg/ml was deposited on the arrays. The microelectrode arrays were then incubated for 1 h at 37 °C, washed three times with PBST, once with PBS, and blocked in 2% (w/v) BSA for 1 h at 37 °C. 6 μl of biotinylated HRP (2.5–25 pM in PBS) were subsequently added and incubated for 15 min at room temperature. All of the modified electrodes were thoroughly washed with PBST and stored in PBS to be immediately used or rinsed with 1% (w/v) trealose before being vacuum-dried for storing at 4 °C.

The lower limit of detection (LOD) of the assays was calculated as the average of at least three blank measurements plus three times their standard deviation.

3. Results and discussion

3.1. Detection of TMB at gold microelectrode arrays

The electrochemistry of TMB^0 has been described by several authors. Broadly speaking, it is a non-toxic aromatic diamine able to reversibly exchange two electrons at an electrode (Volpe et al., 1998; Liu et al., 2008). In this work, we have used a commercial preparation of TMB which is commonly used in ELISA assays. In addition to TMB, this preparation contains H_2O_2 and a series of unknown additives (the supplier would not disclose the composition of the mixture). We chose to use this commercial mixture because the proportions of TMB and H_2O_2 and solvent composition in it have been optimised to provide better signals in the presence of HRP.

Fig. 2a shows the typical cyclic voltammograms (CV) recorded in 200 μl of this commercial TMB/H_2O_2 substrate solution. The two oxidation waves of TMB^0 appear at 0.27 and 0.47 V *vs* Ag/AgCl, respectively. Regardless of scan rate, consecutive CVs obtained from a fresh TMB solution resulted in decreasing peak currents (Fig. 1 in the supplementary data). This was attributed to electrode passivation caused by the precipitation of a charge-transfer complex, CTC, formed by the complexation of the two-electron oxidation product, TMB^{2+}, with the initial TMB^0 present (Misono et al., 1997; Liu et al., 2008). Activating the electrode after each step was thus necessary to achieve reproducibility. In all cases, peak height increases with the square root of scan rate (Fig. 2a, inset), indicating a diffusion-controlled process.

The concentration of TMB^0 in the mixture was estimated to be around 0.5 mM by linear sweep voltammetry at microelectrode arrays (data not shown). This value was obtained from the limiting currents, assuming a diffusion coefficient value of 3.11×10^{-10} m^2 s^{-1}, according to the Wilke–Chang semiempirical method (Wilke and Chang, 1955). In most cases, this approximation is accurate within 10% or better compared to experimental values.

3.2. Electrochemical detection of HRP

Enzymes are used as labels in various assays and biosensors. In the latter case, label capture and target detection occur only in the vicinity of the sensing/transducing surface. However, electrochemical detection at macroelectrodes usually takes place within larger volumes to allow for inclusion of working, reference and counter electrodes. This often implies an unnecessary waste of expensive reagents. Microelectrodes offer better sensitivity and can operate in sample volumes of a few microliters. On the other hand, due to their small size, less material may be immobilised and/or captured on their surface, leading to smaller signals compared with macroelectrodes. We started by studying the electrochemical detection

of HRP at microelectrode arrays in sample volumes below 1 ml using the TMB/H_2O_2 mixture described above. Cyclic voltammetry was performed between −0.4 and +0.5 V at scan rate 10 mV s^{-1} immediately after substrate and HRP mixing, and then 3 and 6 min afterwards. In chronoamperometric measurements, the current at −0.1 V *vs* Ag/AgCl was monitored. A chlorinated Ag wire was initially used both as pseudo-reference and counter electrode. The later incorporation of a Pt counter electrode integrated on the chip generated lower current drifts and more reproducible results.

3.2.1. Detection of HRP in solution

The HRP-catalysed oxidation of TMB is coupled to the H_2O_2 HRP-catalysed reduction as illustrated in Fig. 1a. The reaction generates a blue product, attributed to the formation of the above described CTC (Awano et al., 1990; Misono et al., 1997; Liu et al., 2008). Accordingly, when HRP is added to the TMB/H_2O_2 substrate solution, the reduction and oxidation peaks that characterise the electrochemical response of TMB^0 are substituted by the single peak that distinguishes the CTC. The height of the peak increases with incubation time until saturation is reached (Fig. 2 in the supplementary data), with saturation time depending on the relative amounts of enzyme and substrate present. Below saturation conditions, peak height correlated with enzyme concentration for a fixed substrate concentration. In Fig. 2b we show the CVs recorded for 0–1.6 pM HRP following a 3-min incubation in 10 μl of substrate solution. Signal amplification due to product accumulation during this incubation yields an LOD of 6 fM HRP. The potential shift in the voltammograms shown in Fig. 2b is due to usage of a quasi-reference electrode which surface composition may be affected by adsorption of TMB at higher concentrations. At the same time, the shape of the voltammograms is also affected by the increase of TMB concentration. As the concentration of TMB increases the waves turn into peaks, which is likely due to the adsorption of oxidation products that results in electrode passivation. Interestingly, our data indicate that the activity of HRP can be studied by CV without the need to add acid. This is particularly convenient because acid treatment not only stops the reaction, but it inactivates HRP permanently, preventing its later re-utilization.

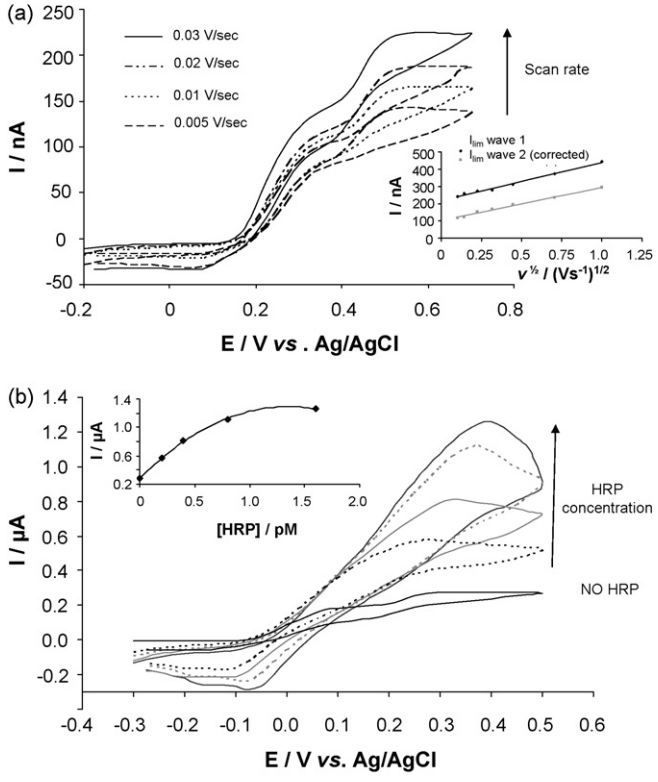

Fig. 2. (a) CVs obtained in TMB/H_2O_2 substrate solution at a gold microelectrode array at increasing scan rates. TMB oxidation generates two oxidation peaks at 0.27 and 0.47 V *vs* a chlorinated silver wire pseudoreference. (*Inset*) Plot of peak height *vs* the square root of the scan rate. (b) CVs obtained in 10 μl TMB/H_2O_2 solution after incubation for 3 min with no HRP, or with 0.2, 0.4, 0.8 and 1.6 pM HRP. (*Inset*) The plot of concentration of HRP *vs* current generated reveals linear correlation in the concentration range 0–0.8 pM.

HRP was also determined chronoamperometrically in two different total solution volumes: 200 and 500 μl of TMB/H_2O_2 substrate solution. Detection was performed at a working potential of −0.1 V *vs* Ag/AgCl, where the background current was negligible and no substrate oxidation occurred. The oxidation of the native TMB^0 was also induced at potentials above 0.1 V *vs* Ag/AgCl, and potentials above +0.3 V resulted in the formation of the CTC, indicated by the appearance in solution of the colour blue even in the absence of HRP. Following signal stabilisation, 1 μl of different HRP concentrated solutions was added to reach final concentrations in the range 1–300 pM. Surprisingly, HRP generated higher currents when measured in the 200 μl volume than it did in 500 μl, despite the fact that the same concentrations of TMB/H_2O_2 were used in both cases. Thus, solutions containing 30 and 60 pM HRP generated currents around 18 and 31 nA respectively when measured in 200 μl volumes compared with 7 and 14 nA in 500 μl volumes. On top of this, detection of lower HRP concentrations was possible in smaller substrate volumes (25 pM of enzyme in 500 *vs* 1 pM in 200 μl of substrate solution respectively; Fig. 3 in the supplementary data). This was unexpected because faradaic currents depend on the concentration of the electroactive species detected and not on sample volume. These differences in signal may be explained by the onset of redox cycling effects (Niwa et al., 1993, 2000) as the distance between working and auxiliary electrodes was shorter in smaller sample volumes. Next we immobilised HRP on the surface of our arrays.

3.2.2. Detection of surface-bound HRP

In the microelectrode arrays used in this work, the sensing surface (gold microdisk electrodes) is physically delimited by an insulating layer of silicon nitride/oxide (Fig. 3a). We observed that biomolecules also adsorbed on this inert cover, and decided to compare the performance of gold devices modified via two different strategies: direct physisorption of biotinylated HRP, and affinity capture using neutravidin.

First, HRP was immobilised by random physisorption directly onto the microelectrode arrays by deposition and incubation of a 10 μl drop of solutions containing 0–10 pM enzyme. This allowed us to carry out chronoamperometric measurements in even lower substrate volumes than before. Fig. 3b shows the average currents registered at four independent electrodes at −0.1 V *vs* Ag/AgCl after addition of just 10 μl of TMB substrate solution. The current recorded increased with the amount of enzyme present on surface until it reached saturation after the chips were incubated in solutions containing 5 pM HRP. The LOD would correspond to incubation of the chips in solutions containing 0.54 pM HRP.

It is difficult to estimate the amount of immobilised HRP because these results cannot be directly compared with those obtained with the enzyme in solution. Incubation of the array in an enzyme solution leads to physisorption of an undetermined quantity of molecules, and only a fraction of them remains active. Therefore the actual surface concentration of active HRP is much lower than that of HRP in the original solution. This is consistent with the low currents registered.

Next, biotinylated HRP was affinity captured on arrays that had been previously modified with neutravidin. The arrays were cleaned, activated, modified with neutravidin and blocked with

BSA as described in the experimental section. Different concentrations of biotinylated HRP were subsequently captured. Negative controls were also performed to determine the levels of enzyme non-specific adsorption (sensor specificity) and background current for each concentration tested. These negative controls used electrodes modified with BSA but without neutravidin, and to which the biotinylated HRP could bind specifically. The arrays were then divided in two subsets. The arrays in the first subset were used in electrochemical measurements without any further preparation. The second sub-set of arrays, on the other hand, were activated following surface modification of the array, so that biomolecules covered only the insulating silicon oxinitride. Freshly activated microelectrodes were expected to show faster electron transfer kinetics and hence better performance. For all the electrodes, the transient currents generated at −0.1 V *vs* Ag/AgCl were recorded for 100 s in 10 μl of substrate.

As revealed in Fig. 3c (light bars), the current registered 5 s after substrate addition for HRP 2.5 and 5 pM was of 10.5 and 12.5 nA on the microelectrode arrays that had been modified on their whole surface (1.6 and 2.4 times the respective negative controls). These signals are significantly higher than those generated in the previous experiment by similar HRP concentrations directly adsorbed onto the chips (3.15 and 3.85 nA). This is consistent with the fact that biomolecules directly physisorbed on a surface tend to denaturate and partially lose functionality. Capture using the appropriate biocomponents has been demonstrated to generate improved performance. HRP 25 pM generated a current of 27 nA, but the signal attributed to enzyme non-specific adsorption was also high (11.7 nA).

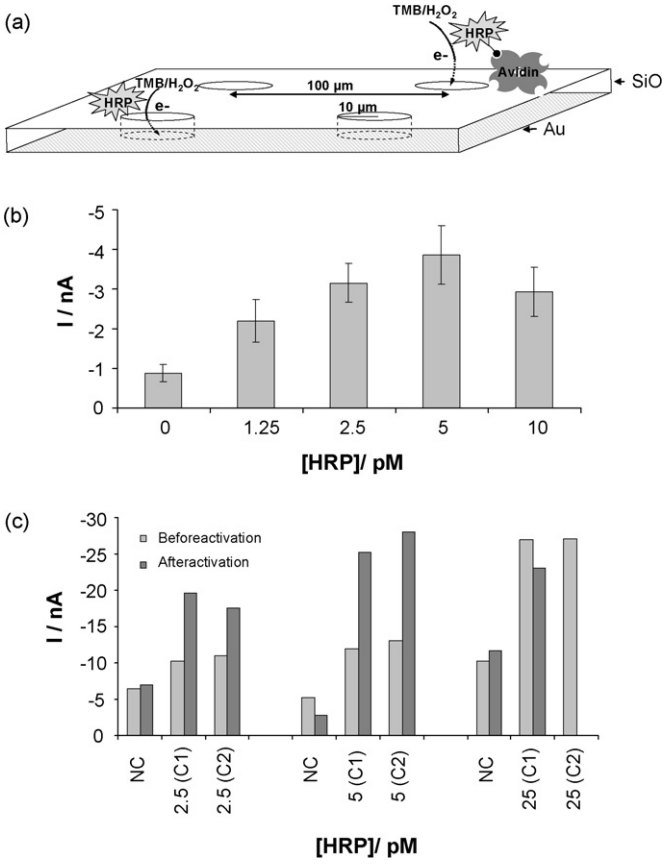

Fig. 3. (a) Two-dimensional section of a microelectrode array. The gold layer is shielded by a silicon oxide/nitride insulating cover, patterned as to expose gold disks. It is used in this work as a physical support for biofunctionalisation and target capture, either by random physisorption (left) or by neutravidin–biotin capture (right). (b) Chronoamperometric detection of directly physisorbed HRP in 10 μl TMB/H_2O_2. Averaged currents recorded on four independent electrodes for each concentration after 5 s of enzyme activity. (c) Chronoamperometric detection of affinity captured HRP in 10 μl TMB/H_2O_2. Light bars: results for electrodes modified onto their whole surface (electrode and non-conducting layer). Dark bars: electrodes that, following modification and HRP capture, had been electrochemically activated (the column 25 (C2) is missing). NC stands for negative control and the C1/C2 columns show values obtained for two independent chips. The coefficient of variation (% CV) was below 8% in all the experiments and for all the conditions tested. The values in the *Y*-axis have been inverted.

When the arrays were electrochemically activated to remove those proteins covering the gold microdisks, the signals registered almost doubled those reported earlier (Fig. 3c, dark bars). HRP 2.5 and 5 pM generated currents of 18.5 and 26.6 nA, which were equivalent to three and nine times the signals generated by the respective negative controls. Under saturating conditions, however, (HRP 25 pM and 10 μl substrate) no differences were observed between data obtained before and after electrode activation. The results obtained confirm that activating the electrodes before measuring leads to better results when microelectrode arrays are used for biosensing. This may seem obvious, but it is actually an important result compared to classical electrochemical biosensing on directly modified macroelectrode surfaces, which cannot be subsequently activated. Hence we believe that microelectrode arrays may lead to better sensitivities relative to conventional biosensors based on macroelectrodes.

Again, in the case of surface immobilised HRP, higher currents were observed when detection was carried out in smaller volumes. The explanation is again thought to be found in redox cycling effects that become more significant with decreasing working-to-auxiliary electrode separation distance. This effect may be further exploited in bipotentiostatic experiments to detect ever lower enzyme concentrations in generator–collector experiments.

3.3. Amperometric detection of H_2O_2 at HRP-functionalised microelectrode arrays

Last, microelectrode arrays featuring immobilised HRP (5 pM) on their inert surface were used to determine H_2O_2 both immediately after modification and following electrochemical activation. In both cases, the electrodes were immersed in 1 ml of 0.2 mM TMB prepared in citrate–phosphate buffer pH 5.0. The current was recorded at −0.1 V until the signal was stable. H_2O_2 was serially diluted in citrate–phosphate buffer and 1 μl of each concentration was successively added to the electrode as to reach final 1–200 μM concentrations. Negative controls were conducted using electrodes that had been washed and activated, but not functionalised with enzyme. The electrodes were then activated and the experiment was repeated.

Fig. 4a shows the currents registered at one of the modified electrodes before and after activation, as well as after treatment for 5 min with 1 M HCl to inactivate the enzyme. Before activation, the surface of the microelectrodes is partly blocked by the proteins making the arrays less sensitive. Under these circumstances the changes in current generated by H_2O_2 addition are so low that the lowest concentrations assayed cannot be detected. Besides, the time required for signal stabilisation following H_2O_2 addition is longer compared to that at the activated electrodes.

When the averaged data recorded for three independent electrodes are studied (Fig. 4b), the differences between activated and not activated electrodes are more evident for the lowest H_2O_2 concentrations tested. For example, the signals registered for 10 and 20 μM H_2O_2 are 15–20 times higher at the activated than at the non-activated arrays, while the signals due to concentrations 50–200 μM are only 2–6 times higher. This might reflect that the higher ratio of TMB^{2+} electroreduction detected at the activated devices generates higher levels of electrode passivation. As already observed in our previous experiments, single measurements pre-

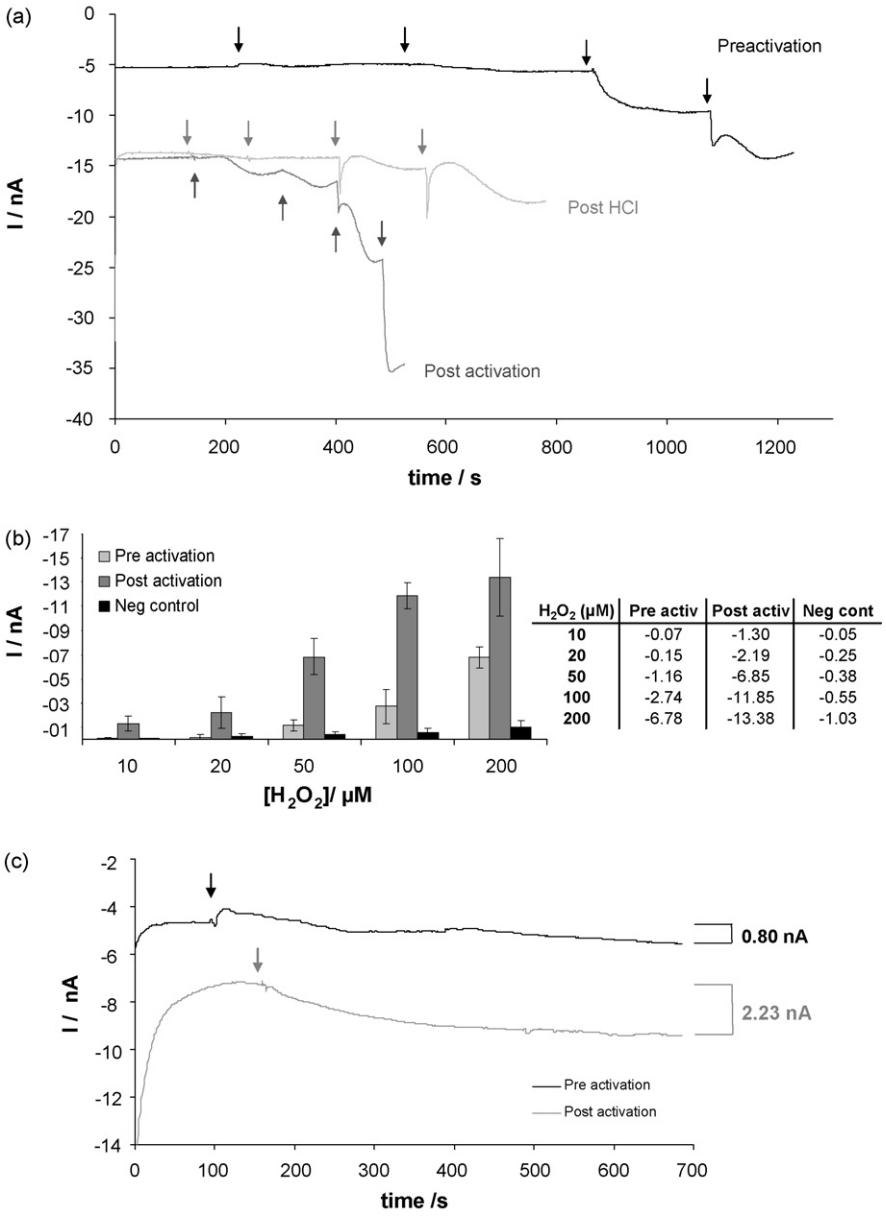

H_2O_2 (µM)	Pre activ	Post activ	Neg cont
10	-0.07	-1.30	-0.05
20	-0.15	-2.19	-0.25
50	-1.16	-6.85	-0.38
100	-2.74	-11.85	-0.55
200	-6.78	-13.38	-1.03

Fig. 4. (a) Chronoamperometric detection of H_2O_2 in 1 ml of TMB at an HRP-modified microelectrode array before and after electrochemical activation, and after enzyme inactivation with 1 M HCl. The arrows indicate addition of H_2O_2 to final concentrations 10, 20, 50 and 100 µM. (b) Increase in current registered for each H_2O_2 concentration before and after activation. The negative controls correspond to electrodes not functionalised with enzyme. Averaged data obtained from at least three independent electrodes. (c) Chronoamperometric detection of 1 µM H_2O_2 in 10 µl of TMB.

ceded by electrode activation would have generated better results. The LOD is of 5.4 µM H_2O_2 at the activated arrays, but it is above 20 µM for the not activated devices.

H_2O_2 detection was also attempted in smaller substrate volumes. Fig. 4c shows as an example the signals recorded at an HRP-modified array in 10 µl of substrate after addition of H_2O_2 to a final concentration of 1 µM. H_2O_2 is detected under these conditions both before and after activation of the electrode, but the change in current recorded is nearly three times higher at the activated device. Thus, as it happened for HRP detection, lessening of the measurement volume improved H_2O_2 detection presumably due to redox cycling effects.

4. Conclusions

Microelectrode arrays are a promising alternative to electrochemical biosensors using macroelectrodes for several reasons. We showed that microfabricated devices allow electrochemical detection in volumes of a few microliters using HRP/H_2O_2 and TMB as a model system. Microelectrode arrays also provide access to lower detection limits, but their most important advantage is that the inert surface between microelectrodes can be used to advantage as a physical support for biofunctionalisation and target capture. There are three reasons for this. The first is that the area where target molecules are captured is much larger than that of the microelectrodes. Second, using integrated but physically separated surfaces for target capture and detection enables the exploitation of complex biofunctionalisation strategies, without negatively affecting signal transduction. This is of extreme importance in the study of real samples where moderate to high loads of organic matter may quickly passivate the electrodes. Third, because this strategy permits that the microelectrodes be activated, so they can keep their electrocatalytic properties intact before substrate addition. In our experiments, detectability at microfabricated

devices that had been functionalised over their entire surface – microdisks included – was poorer than that of the arrays where the microelectrodes had been activated before substrate addition.

Although the approach presented here may be of direct application to most enzyme-based electrochemical bioassays, it also has some limitations. One is variability between arrays, which must be tackled at the fabrication level to ensure that identical areas are available for functionalisation from one array to another. Similarly, biomolecule physisorption is a fast and easy modification strategy but results in random surface coverages. It can be anticipated that using more appropriate surface functionalisation protocols will ensure more reproducible results. Work is in progress to improve surface functionalisation and its reproducibility. Additionally, some of our data also suggest that microelectrode arrays may facilitate the design of generator–collector experiments that allow for even better sensitivities.

Acknowledgments

This work has been funded by the project DPS2008-07005-C02-02 from the Spanish Ministry of Science and Innovation. E. Baldrich and F. Javier del Campo are respectively supported by an I3P fellowship from the Consejo Superior de Investigaciones Científicas (CSIC, Spain) and a Ramón y Cajal fellowship from the Spanish Ministry of Education.

Appendix A. Supplementary data

Supplementary data associated with this article can be found, in the online version, at doi:10.1016/j.bios.2009.09.009.

References

Awano, H., Ogata, T., Murakami, H., Yamashita, T., Ohigashi, H., 1990. Synth. Met. 36 (2), 263–266.
Baldrich, E., Acero, J.L., Reekmans, G., Laureyn, W., O'Sullivan, C.K., 2005. Anal. Chem. 77 (15), 4774–4784.
Butler, D., Pravda, M., Guilbault, G.G., 2006. Anal. Chim. Acta 556 (2), 333–339.
Conneely, G., Aheerne, M., Lu, H.H., Guilbault, G.G., 2007. Sens. Actuator B Chem. 121 (1), 103–112.
Crew, A., Alford, C., Cowell, D.C.C., Hart, J.P., 2007. Electrochim. Acta 52 (16), 5232–5237.
Davies, T.J., Ward-Jones, S., Banks, C.E., del Campo, J., Mas, R., Munoz, F.X., Compton, R.G., 2005. J. Electroanal. Chem. 585 (1), 51–62.
Draisci, R., delli Quadri, F., Achene, L., Volpe, G., Palleschi, L., Palleschi, G., 2001. Analyst 126 (11), 1942–1946.
Fanjul-Bolado, P., Gonzalez-Garia, M.B., Costa-Garcia, A., 2005. Anal. Bioanal. Chem. 382 (2), 297–302.
He, Y.N., Chen, H.Y., Zheng, J.J., Zhang, G.Y., Chen, Z.L., 1997. Talanta 44 (5), 823–830.
He, Z.H., Gao, N., Jin, W.R., 2003. Anal. Chim. Acta 497 (1–2), 75–81.
Josephy, P.D., Eling, T., Mason, R.P., 1982. J. Biol. Chem. 257 (7), 3669–3675.
Kricka, L.J., 1994. Clin. Chem. 40 (3), 347–357.
Kurtinaitiene, B., Ambrozaite, D., Laurinavicius, V., Ramanaviciene, A., Ramanavicius, A., 2008. Biosens. Bioelectron. 23 (10), 1547–1554.
Liu, G.D., Riechers, S.L., Timchalk, C., Lin, Y.H., 2005. Electrochem. Commun. 7 (12), 1463–1470.
Liu, G.D., Timchalk, C., Lin, Y.H., 2006. Electroanalysis 18 (16), 1605–1613.
Liu, M.L., Zhang, Y.Y., Chen, Y.D., Xie, Q.J., Yao, S.Z., 2008. J. Electroanal. Chem. 622 (2), 184–192.
Lu, H.H., Kreuzer, M.P., Takkinen, K., Guilbault, G.G., 2007. Biosens. Bioelectron. 22 (8), 1756–1763.
Misono, Y., Ohkata, Y., Morikawa, T., Itoh, K., 1997. J. Electroanal. Chem. 436 (1–2), 203–212.
Niwa, O., Kurita, R., Liu, Z.M., Horiuchi, T., Torimitsue, K., 2000. Anal. Chem. 72 (5), 949–955.
Niwa, O., Xu, Y., Halsall, H.B., Heineman, W.R., 1993. Anal. Chem. 65 (11), 1559–1563.
Ordeig, O., Banks, C.E., Davies, T.J., del Campo, J., Mas, R., Munoz, F.X., Compton, R.G., 2006. Analyst 131 (3), 440–445.
Ordeig, O., del Campo, J., Munoz, F.X., Banks, C.E., Compton, R.G., 2007. Electroanalysis 19 (19–20), 1973–1986.
Parker, C.O., Tothill, I.E., 2009. Biosens. Bioelectron. 24 (8), 2452–2457.
Pyun, J.C., Lee, H.H., Lee, C.S., 2001. Sens. Actuator B Chem. 78 (1–3), 232–236.
Regalado, C., Garciïa-Almendaĭrez, B.E., Duarte-Vazquez, M.A., 2004. Phytochem. Rev. 3 (1–2), 243–256.
Salam, F., Tothill, I.E., 2009. Biosens. Bioelectron. 24 (8), 2630–2636.
Valentini, F., Compagnone, D., Giraudi, G., Palleschi, G., 2003. Anal. Chim. Acta 487 (1), 83–90.
Veitch, N.C., 2004. Phytochemistry 65 (3), 249–259.
Volpe, G., Compagnone, D., Draisci, R., Palleschi, G., 1998. Analyst 123 (6), 1303–1307.
Wilke, C.R., Chang, P., 1955. AIChE J. 1 (2), 264–270.
Zhou, Y.M., Hu, S.Q., Shen, G.L., Yu, R.Q., 2003. Biosens. Bioelectron. 18 (4), 473–481.